Delft University of Technology

Delft Center for Systems and Control

Technical report 10-048

Integrated urban traffic control for the reduction of travel delays and emissions*

S. Lin, B. De Schutter, S.K. Zegeye, H. Hellendoorn, and Y. Xi

If you want to cite this report, please use the following reference instead:

S. Lin, B. De Schutter, S.K. Zegeye, H. Hellendoorn, and Y. Xi, "Integrated urban traffic control for the reduction of travel delays and emissions," *Proceedings of the 13th International IEEE Conference on Intelligent Transportation Systems (ITSC 2010)*, Madeira Island, Portugal, pp. 677–682, Sept. 2010. doi:10.1109/ITSC.2010.5625020

Delft Center for Systems and Control
Delft University of Technology
Mekelweg 2, 2628 CD Delft
The Netherlands
phone: +31-15-278.24.73 (secretary)
URL: https://www.dcsc.tudelft.nl

*This report can also be downloaded via https://pub.bartdeschutter.org/abs/10_048.html

Integrated urban traffic control for the reduction of travel delays and emissions

Shu Lin, Bart De Schutter, Solomon K. Zegeye, Hans Hellendoorn, and Yugeng Xi

***Abstract*— An integrated macroscopic traffic model is proposed, which integrates a macroscopic urban traffic flow model with a microscopic traffic emission model for individual vehicles. As a macroscopic model, the integrated model is fast enough for on-line control purposes. Nevertheless, the model can still capture the traffic emissions for vehicles in different states compared with using a macroscopic traffic emission model, because of the accuracy of the microscopic traffic emission model. Model Predictive Control is applied to control urban traffic areas based on the integrated traffic model, aiming at reducing both travel delays and traffic emissions.**

I. Introduction

One of the biggest sources of the environmental pollution in cities comes from the emissions of the busy traffic flows. The emissions of vehicles contain several harmful substances, like nitrogen (monoxide, dioxide, etc., i.e. NO_x), hydrocarbons (HC), carbon monoxide (CO), carbon dioxide (CO_2), etc. Therefore, it is very necessary to integrate traffic emissions control into the urban traffic management system, so as to provide a healthier and safer living environment for the people living in urban areas.

So far, most of the ongoing research is focusing on reducing traffic delays and traffic congestion, and improving the traffic flow throughput. However, in some circumstances, an increased traffic flow throughput may result in even higher total traffic emissions [1]. In general, we cannot take for granted that the smaller travel delay is, the less traffic emissions will be generated. In fact, the emissions of a vehicle depend greatly on the operational conditions of the vehicle [2]–[4]. Large emissions can be given out by a vehicle with either too high speed or too low speed. Therefore, an integrated control strategy is necessary that balances performance in terms of both travel delays and all types of traffic emissions. Traffic control strategies considering both travel delays and traffic emissions for highways have already been discussed [1], [5], [6]. In this paper we will address this problem for urban areas.

Model Predictive Control (MPC) [7] is an advanced control method that can satisfy the requirements for this control problem. In this paper, a macroscopic urban traffic model which also estimates the emissions of traffic flows is proposed, and an MPC controller considering both traffic delays and emissions is built using this model as the prediction model. Since each step the MPC controller on-line solves an optimization problem, it has high requirements for the on-line computational complexity of the prediction model. The S model [8], [9] is taken as the prediction model for the MPC controller. This model is a macroscopic urban traffic model, which is fast to compute and also accurate enough for control purposes [8]. In order to well capture the emissions of a vehicle running on a road in urban area, a microscopic traffic emission model, which is based on both velocity and acceleration, is selected. This vehicle emission model provides reasonable estimates, when the vehicle is decelerating, accelerating, or moving slowly in front of the stop-line in red signals. Integrated with this microscopic traffic emission model, the overall macroscopic prediction model is able to provide estimations of both travel delays and emissions for the MPC controller.

S. Lin, B. De Schutter, S. K. Zegeye, and J. Hellendoorn are with the Delft Center for Systems and Control, Delft University of Technology, The Netherlands. {s.lin, b.deschutter, s.k.zegeye, j.hellendoorn}@tudelft.nl

S. Lin and Y. Xi are with Department of Automation, Shanghai Jiao Tong University, Shanghai, China. lisashulin@gmail.com, ygxi@sjtu.edu.cn

II. Macroscopic urban traffic model (S model)

In the macroscopic urban traffic model of [8], called the S model, we define J the set of nodes (intersections), and L the set of links (roads) in the urban traffic network. A link (u,d) is marked by its upstream node u $(u \in J)$ and downstream node d $(d \in J)$. The input and output links of link (u,d) can be also specified by this upstream and downstream nodes. The sets of input and output nodes for link (u,d) are $I_{u,d} \subset J$ and $O_{u,d} \subset J$.

In order to describe the evolution of the models, we first define some variables:

- $I_{u,d}$: set of input nodes of link (u,d),
- $O_{u,d}$: set of output nodes of link (u,d),
- k_d : simulation step counter,
- $n_{u,d}(k_d)$: number of vehicles in link (u,d) at step k_d,
- $q_{u,d}(k_d)$: queue length at step k_d in link (u,d); $q_{u,d,o}$ is the queue length of the sub-stream turning to link o,
- $\alpha^{\text{leave}}_{u,d}(k_d)$: flow rate leaving link (u,d) at step k_d; $\alpha^{\text{leave}}_{u,d,o}(k_d)$ is the leaving flow rate of the sub-stream towards o,
- $\alpha^{\text{arriv}}_{u,d}(k_d)$: flow rate arriving at the end of the queue in link (u,d) at step k_d; $\alpha^{\text{arriv}}_{u,d,o}(k_d)$ is the arriving flow rate of the sub-stream towards o,
- $\alpha^{\text{enter}}_{u,d}(k_d)$: flow rate entering link (u,d) at step k_d; $\alpha^{\text{enter}}_{i,u,d}(k_d)$ is the flow rate entering link (u,d) from i,
- $\beta_{u,d,o}(k_d)$: relative fraction of the traffic on link (u,d) turning to o at step k_d,

$\mu_{u,d}$: saturated flow rate leaving link (u,d),
$g_{u,d,o}(k_d)$: green time length during step k_d for the traffic stream towards o in link (u,d),
$v_{u,d}^{\text{free}}$: free-flow vehicle speed in link (u,d),
$C_{u,d}$: capacity of link (u,d) expressed in number of vehicles,
$N_{u,d}^{\text{lane}}$: number of lanes in link (u,d),
$\Delta c_{u,d}$: offset between node u and node d, which represents the offset time between the cycle times of the upstream and the downstream intersections at the beginning of every control time step,
l_{veh} : average vehicle length.

In the S model, every intersection takes the cycle time as its simulation time interval. The cycle times for intersections u and d, which are denoted by c_u and c_d respectively, can be different from each other. In this situation, the simulation step counters of different intersections are not same. As cycle times are the simulation time intervals of the S model, the input and output flow rates of the link are averaged over the cycle times in the S model.

Taking the cycle time c_d as the length of the simulation time interval for link (u,d) and k_d as the corresponding time step counter, the number of the vehicles in link (u,d) is updated according to the input and output average flow rate over c_d at every time step k_d by

$$n_{u,d}(k_d+1) = n_{u,d}(k_d) + \left(\alpha_{u,d}^{\text{enter}}(k_d) - \alpha_{u,d}^{\text{leave}}(k_d)\right)\cdot c_d \quad . \quad (1)$$

The leaving flow rate $\alpha_{u,d}^{\text{leave}}(k_d)$ is the sum of the leaving flow rates $\alpha_{u,d,o}^{\text{leave}}(k_d)$ turning to each output link $o \in O_{u,d}$.

The leaving average flow rate over c_d is determined by the capacity of the intersection, the number of cars waiting and arriving, and the available space in the downstream link:

$$\begin{aligned}\alpha_{u,d,o}^{\text{leave}}(k_d) = \min\Big(&\beta_{u,d,o}(k_d)\cdot\mu_{u,d}\cdot g_{u,d,o}(k_d)/c_d, \\ &q_{u,d,o}(k_d)/c_d + \alpha_{u,d,o}^{\text{arriv}}(k_d), \\ &\beta_{u,d,o}(k_d)\left(C_{d,o} - n_{d,o}(k_d)\right)/c_d\Big) \quad .\end{aligned} \quad (2)$$

The number of vehicles waiting in the queue turning to link o is updated as

$$q_{u,d,o}(k_d+1) = q_{u,d,o}(k_d) + \left(\alpha_{u,d,o}^{\text{arriv}}(k_d) - \alpha_{u,d,o}^{\text{leave}}(k_d)\right)\cdot c_d \quad . \quad (3)$$

The flow of vehicles that entered link (u,d) will arrive at the end of the queues after a time delay $\tau(k_d)\cdot c_d + \gamma(k_d)$:

$$\begin{aligned}\alpha_{u,d}^{\text{arriv}}(k_d) = &\frac{c_d - \gamma(k_d)}{c_d}\alpha_{u,d}^{\text{enter}}(k_d - \tau(k_d)) + \\ &\frac{\gamma(k_d)}{c_d}\alpha_{u,d}^{\text{enter}}(k_d - \tau(k_d) - 1),\end{aligned} \quad (4)$$

with

$$\begin{aligned}\tau(k_d) &= \text{floor}\left\{\frac{\left(C_{u,d} - q_{u,d}(k_d)\right)\cdot l_{\text{veh}}}{N_{u,d}^{\text{lane}}\cdot v_{u,d}^{\text{free}}\cdot c_d}\right\}, \\ \gamma(k_d) &= \text{rem}\left\{\frac{\left(C_{u,d} - q_{u,d}(k_d)\right)\cdot l_{\text{veh}}}{N_{u,d}^{\text{lane}}\cdot v_{u,d}^{\text{free}}\cdot c_d}\right\}.\end{aligned} \quad (5)$$

When reaching the end of the link, the arriving flow rate is separated into sub-streams by multiplying it with the turning rate $\beta_{u,d,o}(k_d)$.

The flow rate entering link (u,d) is the sum of the flow rates entering from all the upstream links:

$$\alpha_{u,d}^{\text{enter}}(k_d) = \sum_{i\in I_{u,d}}\alpha_{i,u,d}^{\text{enter}}(k_d) = \sum_{i\in I_{u,d}}\alpha_{i,u,d}^{\text{leave}}(k_u). \quad (6)$$

Some operations need to be carried out to synchronize the leaving and entering flow rates. This goes as follows [8]: A common control time interval is adopted by all the intersections in the network, with N_j an integer, as

$$T_{\text{c}} = N_j\cdot c_j, \quad \text{for all } j\in J \ , \quad (7)$$

where T_{c} is the least common multiple of all the intersection cycle times in the traffic network, which ensures all the intersections can communicate with each other and be synchronized.

The leaving flow rates in the timing of intersection u can be recast into the entering flow rates in the timing of intersection d as follows. First, we transform the discrete-time leaving flow rates from the upstream links into continuous time using a zero-order hold strategy, as

$$\alpha_{i,u,d}^{\text{leave,cont}}(t) = \alpha_{i,u,d}^{\text{leave}}(k_u), \quad k_u\cdot c_u \le t < (k_u+1)\cdot c_u, \quad (8)$$

and then we convert the result again to obtain the average entering flow rates in time step k_d so as to make them can be used by the downstream link as follows

$$\alpha_{i,u,d}^{\text{enter}}(k_d) = \frac{\displaystyle\int_{k_d\cdot c_d+\Delta c_{u,d}}^{(k_d+1)\cdot c_d+\Delta c_{u,d}}\alpha_{i,u,d}^{\text{leave,cont}}(t)}{c_d}\,\text{d}t \quad . \quad (9)$$

III. Microscopic traffic emission model

Vehicle emissions depend on many factors, such as vehicle status (like engine, age, and maintenance), environmental conditions (such as infrastructure and weather), and operational factors (such as speed, acceleration, and engine load). These last factors are the most decisive elements for the fuel consumption and the emission of harmful substances.

There are two types of emission and fuel consumption models: average-speed-based models and dynamic-based models. Average-speed-based models calculate the emissions and fuel consumption of each vehicle based on the average traveling speed of the vehicle. This average traveling speed can be calculated either over the entire trip, or over some local time periods to take some variations of the speed into consideration. On the contrary, dynamic-based models use more detailed knowledge of the vehicle dynamics, i.e. the speed and acceleration data of each vehicle at every time instant. As they are microscopic traffic emission and fuel consumption models, dynamic-based models are more accurate than the average-speed-based models.

VT-micro [2] is a microscopic dynamic-based traffic emission and fuel consumption model. It evaluates the emissions based on not only the speed of every vehicle, but also the acceleration or the deceleration of each vehicle. The traffic

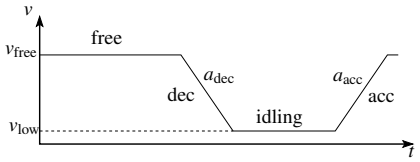

(a) Vehicle dynamic behavior on a road with a stop

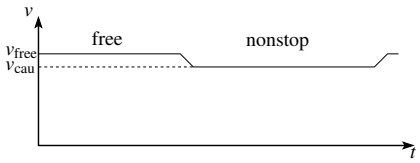

(b) Vehicle dynamic behavior on a road without any stops

Fig. 1. Vehicle dynamic behavior on a road

emissions can be calculated even when a vehicle stops at the stop line or starts up to leave from the stop line. These behaviors are the typical states of vehicles while they are traveling within urban areas. Therefore, VT-micro is selected as the emission model for the vehicles. VT-micro generates emissions of an individual vehicle with index i at every time step k based on the current speed $v_i(k)$ and acceleration $a_i(k)$ of the vehicle, as

$$E_{\theta,i}(v_i(k),a_i(k)) = \exp(\tilde{\mathbf{v}}_i^{\mathrm{T}}(k)\mathbf{P}_\theta\tilde{\mathbf{a}}_i(k)), \tag{10}$$

where $E_{\theta,i}$ stands for the emission $\theta \in M = \{\mathrm{CO},\mathrm{CO_2},\mathrm{NO}_x,\mathrm{HC}\}$, and the vectors of velocity and acceleration are defined as $\tilde{\mathbf{v}}_i(k) = [1\ v_i(k)\ v_i^2(k)\ v_i^3(k)]^{\mathrm{T}}$, $\tilde{\mathbf{a}}_i(k) = [1\ a_i(k)\ a_i^2(k)\ a_i^3(k)]^{\mathrm{T}}$, while $\mathbf{P}_\theta$ is the parameter matrix for emission type θ (see [2], [6]).

IV. Integrated traffic flow and traffic emission model

A. Urban traffic behaviors for individual vehicles

As a microscopic model, the VT-micro model provides the emissions of an individual vehicle at a certain location and a time instant. But, as a macroscopic model, the S model only provides information of traffic flows instead of every detail of every individual vehicle. However, the S model can capture the main behavior of the vehicles, when they are running along a road. The time period spent by a vehicle running along a road can be divided into several parts, in each of which the behavior of the vehicle is assumed to be uniform. Define the set of the behaviors as $B = \{\text{free},\text{idling},\text{dec},\text{acc},\text{nonstop}\}$. Fig. 1 shows how the velocity of a vehicle could vary in different behavior regions, when it travels along an urban road.

As Fig. 1(a) shows, in the regions "free" and "idling", the vehicle runs with a constant velocity, i.e. the acceleration is $a = 0$. The region "free" stands for the time period that the vehicle is running on the link with free-flow speed $v = v_{\text{free}}$, while the region "idling" represents the time period that the vehicle is moving in a queue in front of an intersection with a very low speed $v = v_{\text{low}}$. Therefore, the emission functions for the vehicle running with free-flow speed and the vehicle idling with a very low speed in the queues are respectively

$$E_{\theta,i}^{\text{free}}(k) = E_{\theta,i}(v_{\text{free}},0), \tag{11}$$

$$E_{\theta,i}^{\text{idling}}(k) = E_{\theta,i}(v_{\text{low}},0). \tag{12}$$

The regions "dec" and "acc" respectively represent the deceleration and acceleration behavior of the vehicle near an intersection. Here, the assumption is made that the vehicle will decelerate and accelerate with constant acceleration $a_{\text{dec}} < 0$ and $a_{\text{acc}} > 0$ respectively. The average velocity v_{avrg} is used in the emission function to approximate the velocity during decelerating and accelerating. Then, the emission functions for the vehicle decelerating and accelerating are

$$E_{\theta,i}^{\text{dec}}(k) = E_{\theta,i}(v_{\text{avrg}},a_{\text{dec}}), \tag{13}$$

$$E_{\theta,i}^{\text{acc}}(k) = E_{\theta,i}(v_{\text{avrg}},a_{\text{acc}}), \tag{14}$$

where the average velocity of the vehicle is an average of the velocity before and after acceleration: $v_{\text{avrg}} = (v_{\text{free}} + v_{\text{low}})/2$.

If the vehicle arrives at the stop line, where no queue is in front of it and the traffic light is also green, then the vehicle will leave the link without a stop at a constant speed. This constant speed, v_{cau}, is a little bit lower than the free-flow speed, because drivers will be more cautious while passing the intersections. Therefore, the emissions for the nonstop vehicles are (see Fig. 1(b))

$$E_{\theta,i}^{\text{nonstop}}(k) = E_{\theta,i}(v_{\text{cau}},0). \tag{15}$$

B. Integrated VT-S traffic emission model

The S model provides macroscopic traffic states for each link $(u,d) \in L$ in each simulation time interval (cycle time). The traffic states include the number of vehicles traveling with free-flow speed, the number of vehicles decelerating and accelerating, the number of vehicle waiting in queues. Based on this macroscopic information and the microscopic emission model of the previous section, a macroscopic traffic emission model can be obtained by combining the macroscopic S model and the VT-micro model together, which results in a macroscopic integrated traffic flow and emission model, which we call the VT-S model.

The VT-S model for emission x of link $(u,d) \in L$ during time period $[c_d \cdot k_d, c_d \cdot (k_d+1)]$ is

$$\begin{aligned} E_{\theta,u,d}(k_d) &= \sum_{b\in B}\sum_{k\in\mathscr{K}(b,u,d,k_d)}\sum_{i\in\mathscr{V}(b,u,d,k)} E_{\theta,u,d,i}^{b}(k) \\ &= \sum_{b\in B} E_{\theta,u,d}^{b}(k_d)\cdot N_{u,d}^{b}(k_d)\cdot\frac{c_d}{T}\cdot\frac{t_{u,d}^{b}(k_d)}{c_d}, \end{aligned} \tag{16}$$

where $\mathscr{V}(b,u,d,k)$ is the set of vehicles that have behavior b at time step k in link (u,d), $\mathscr{K}(b,u,d,k_d)$ is the set of time steps $kT \in [c_d \cdot k_d, c_d \cdot (k_d+1)]$ at which the vehicles are in behavior b in link (u,d), $E_{\theta,u,d}^{\mathrm{b}}(k_d)$ is the constant traffic emission for emission x of a vehicle on link (u,d) with behavior b during time period $[c_d \cdot k_d, c_d \cdot (k_d+1)]$, $N_{u,d}^{b}(k_d)$ is the number of vehicles that have behavior b in link u,d during time period $[c_d \cdot k_d, c_d \cdot (k_d+1)]$, and $t_{u,d}^{b}(k_d)$ is the time period that the vehicles keep having this behavior.

Urban traffic states on a link can be separated into different scenarios according to the level of the traffic density. In the saturated traffic scenario, the queues of vehicles resulting from the red phase cannot be dissolved completely at the following green phase, i.e. all the arriving vehicles have to stop and wait once for the next green light to leave the link. For the over-saturated traffic scenario, the vehicles need to wait for even more cycle times in the queues than in saturated scenario. On the contrary, in the unsaturated traffic scenario, all the accumulated vehicles during the red phase are able to leave the link in the following green phase, some vehicles can even leave the link without any stop. Since the traffic behaviors could differ between these scenarios, the VT-S model can be further illustrated respectively for the three scenarios.

1) Saturated scenario: In the saturated scenario, not all the vehicles waiting and arriving in the queues could leave the link in the current green phase, some vehicles have to wait until the next green phase, i.e. the number of vehicles waiting and arriving to leave the link exceeds the maximum number of vehicles that could leave at most in one cycle time, but the queues can be dissolved in the current green phase. This is characterized by the following condition:

$$q_{u,d}(k_d) \leq \sum_{o \in O_{u,d}} \beta_{u,d,o}(k_d) \cdot \mu_{u,d} \cdot g_{u,d,o}(k_d) \leq c_d \cdot \alpha_{u,d}^{\text{arriv}}(k_d) + q_{u,d}(k_d)\,. \tag{17}$$

So, all the vehicles have to wait once for a red traffic signal in the queues before leaving the link, i.e. no vehicle can leave the link without stop. For the saturated scenario, the number of vehicles that have behavior $b \in B$ in link (u,d) during time period $[c_d \cdot k_d, c_d \cdot (k_d+1)]$ is given by

$$N_{u,d}^{\text{free}}(k_d) = n_{u,d}(k_d) - c_d \cdot \alpha_{u,d}^{\text{arriv}}(k_d) - q_{u,d}(k_d) \tag{18}$$

$$N_{u,d}^{\text{idling},1}(k_d) = c_d \cdot \alpha_{u,d}^{\text{arriv}}(k_d) + q_{u,d}(k_d) - \tag{19}$$

$$\sum_{o \in O_{u,d}} \beta_{u,d,o}(k_d) \cdot \mu_{u,d} \cdot g_{u,d,o}(k_d) \tag{20}$$

$$N_{u,d}^{\text{idling},2}(k_d) = \sum_{o \in O_{u,d}} \beta_{u,d,o}(k_d) \cdot \mu_{u,d} \cdot g_{u,d,o}(k_d) - q_{u,d}(k_d) \tag{21}$$

$$N_{u,d}^{\text{idling},3}(k_d) = 0 \tag{22}$$

$$N_{u,d}^{\text{idling},4}(k_d) = q_{u,d}(k_d) \tag{23}$$

$$N_{u,d}^{\text{dec}}(k_d) = c_d \cdot \alpha_{u,d}^{\text{arriv}}(k_d) \tag{24}$$

$$N_{u,d}^{\text{acc}}(k_d) = \sum_{o \in O_{u,d}} \beta_{u,d,o}(k_d) \cdot \mu_{u,d} \cdot g_{u,d,o}(k_d) \tag{25}$$

$$N_{u,d}^{\text{nonstop}}(k_d) = 0\,, \tag{26}$$

and the time periods that the vehicles keep having this behavior during time period $[c_d \cdot k_d, c_d \cdot (k_d+1)]$ are

$$t_{u,d}^{\text{free}}(k_d) = c_d \tag{27}$$

$$t_{u,d}^{\text{idling},1}(k_d) = c_d - (v_{\text{low}} - v_{\text{free}})/a_{\text{dec}} \tag{28}$$

$$t_{u,d}^{\text{idling},2}(k_d) = c_d - (v_{\text{low}} - v_{\text{free}})/a_{\text{dec}} - (v_{\text{free}} - v_{\text{low}})/a_{\text{acc}} \tag{29}$$

$$t_{u,d}^{\text{idling},3}(k_d) = 0 \tag{30}$$

$$t_{u,d}^{\text{idling},4}(k_d) = c_d - (v_{\text{free}} - v_{\text{low}})/a_{\text{acc}} \tag{31}$$

$$t_{u,d}^{\text{dec}}(k_d) = (v_{\text{low}} - v_{\text{free}})/a_{\text{dec}} \tag{32}$$

$$t_{u,d}^{\text{acc}}(k_d) = (v_{\text{free}} - v_{\text{low}})/a_{\text{acc}} \tag{33}$$

$$t_{u,d}^{\text{nonstop}}(k_d) = 0\,. \tag{34}$$

2) Over-saturated scenario: In the over-saturated scenario, the vehicles waiting in the queues could not leave the link in the current green phase. Hence, the number of vehicles waiting in the queues to leave the link exceeds the maximum number of vehicles that could leave at most in one cycle time:

$$\sum_{o \in O_{u,d}} \beta_{u,d,o}(k_d) \cdot \mu_{u,d} \cdot g_{u,d,o}(k_d) < q_{u,d}(k_d)\,. \tag{35}$$

For the over-saturated scenario, the number of vehicles having behavior $b \in B$ during $[c_d \cdot k_d, c_d \cdot (k_d+1)]$ is

$$N_{u,d}^{\text{free}}(k_d) = n_{u,d}(k_d) - c_d \cdot \alpha_{u,d}^{\text{arriv}}(k_d) - q_{u,d}(k_d) \tag{36}$$

$$N_{u,d}^{\text{idling},1}(k_d) = c_d \cdot \alpha_{u,d}^{\text{arriv}}(k_d) \tag{37}$$

$$N_{u,d}^{\text{idling},2}(k_d) = 0 \tag{38}$$

$$N_{u,d}^{\text{idling},3}(k_d) = q_{u,d}(k_d) - \sum_{o \in O_{u,d}} \beta_{u,d,o}(k_d) \cdot \mu_{u,d} \cdot g_{u,d,o}(k_d) \tag{39}$$

$$N_{u,d}^{\text{idling},4}(k_d) = \sum_{o \in O_{u,d}} \beta_{u,d,o}(k_d) \cdot \mu_{u,d} \cdot g_{u,d,o}(k_d) \tag{40}$$

$$N_{u,d}^{\text{dec}}(k_d) = c_d \cdot \alpha_{u,d}^{\text{arriv}}(k_d) \tag{41}$$

$$N_{u,d}^{\text{acc}}(k_d) = \sum_{o \in O_{u,d}} \beta_{u,d,o}(k_d) \cdot \mu_{u,d} \cdot g_{u,d,o}(k_d) \tag{42}$$

$$N_{u,d}^{\text{nonstop}}(k_d) = 0\,, \tag{43}$$

and the time periods that the vehicles keep having this behavior in link (u,d) are given by

$$t_{u,d}^{\text{free}}(k_d) = c_d \tag{44}$$

$$t_{u,d}^{\text{idling},1}(k_d) = c_d - (v_{\text{low}} - v_{\text{free}})/a_{\text{dec}} \tag{45}$$

$$t_{u,d}^{\text{idling},2}(k_d) = 0 \tag{46}$$

$$t_{u,d}^{\text{idling},3}(k_d) = c_d \tag{47}$$

$$t_{u,d}^{\text{idling},4}(k_d) = c_d - (v_{\text{free}} - v_{\text{low}})/a_{\text{acc}} \tag{48}$$

$$t_{u,d}^{\text{dec}}(k_d) = (v_{\text{low}} - v_{\text{free}})/a_{\text{dec}} \tag{49}$$

$$t_{u,d}^{\text{acc}}(k_d) = (v_{\text{free}} - v_{\text{low}})/a_{\text{acc}} \tag{50}$$

$$t_{u,d}^{\text{nonstop}}(k_d) = 0\,. \tag{51}$$

3) Unsaturated scenario: In the unsaturated scenario, the queues can be dissolved before the current green phase ends. Thus, the traffic demand, i.e. the number of vehicles waiting and arriving to leave the link is less than the maximum number of vehicles that could leave in one cycle time, which is characterized as

$$c_d \cdot \alpha_{u,d}^{\text{arriv}}(k_d) + q_{u,d}(k_d) < \sum_{o \in O_{u,d}} \beta_{u,d,o}(k_d) \cdot \mu_{u,d} \cdot g_{u,d,o}(k_d)\,. \tag{52}$$

Therefore, during a green phase, the vehicles waiting in the queues can be considered to first leave the link according to the saturated flow rate of the link $\mu_{u,d}$, and then, after the queues are dissolved, the arriving vehicles will leave the link without a stop according to the arriving (or demand) flow rate $\alpha^{\text{arriv}}_{u,d}(k_d)$ in the rest of the green time. Hereafter, the green time for link (u,d) in the k_d th cycle time, $g_{u,d}(k_d)$, can be approximately separated into two parts, one is green time $g^{\text{s}}_{u,d}(k_d)$ in which the traffic leaves the link with the saturated flow rate, the other is green time $g^{\text{d}}_{u,d}(k_d)$ during which the traffic leaves the link with the demand flow rate. The quantities of $g^{\text{s}}_{u,d}(k_d)$ and $g^{\text{d}}_{u,d}(k_d)$ satisfy

$$\begin{aligned} &c_d\alpha^{\text{arriv}}_{u,d}(k_d)+q_{u,d}(k_d)=g^{\text{s}}_{u,d}(k_d)\mu_{u,d}+g^{\text{d}}_{u,d}(k_d)\alpha^{\text{arriv}}_{u,d}(k_d)\\ &g^{\text{s}}_{u,d}(k_d)+g^{\text{d}}_{u,d}(k_d)=g_{u,d}(k_d)\,. \end{aligned} \tag{53}$$

Hence, we have

$$g^{\text{s}}_{u,d}(k_d)=\frac{c_d\alpha^{\text{arriv}}_{u,d}(k_d)+q_{u,d}(k_d)-g_{u,d}(k_d)\alpha^{\text{arriv}}_{u,d}(k_d)}{\mu_{u,d}-\alpha^{\text{arriv}}_{u,d}(k_d)} \tag{54}$$

$$g^{\text{d}}_{u,d}(k_d)=\frac{g_{u,d}(k_d)\mu_{u,d}-c_d\alpha^{\text{arriv}}_{u,d}(k_d)-q_{u,d}(k_d)}{\mu_{u,d}-\alpha^{\text{arriv}}_{u,d}(k_d)}\,. \tag{55}$$

For the unsaturated scenario, the number of vehicles that have behavior $b\in B$ in link (u,d) $[c_d\cdot k_d, c_d\cdot(k_d+1)]$ is

$$N^{\text{free}}_{u,d}(k_d)=n_{u,d}(k_d)-c_d\cdot\alpha^{\text{arriv}}_{u,d}(k_d)-q_{u,d}(k_d) \tag{56}$$

$$N^{\text{idling},1}_{u,d}(k_d)=0 \tag{57}$$

$$N^{\text{idling},2}_{u,d}(k_d)=(c_d-g^{\text{d}}_{u,d}(k_d))\alpha^{\text{arriv}}_{u,d}(k_d) \tag{58}$$

$$N^{\text{idling},3}_{u,d}(k_d)=0 \tag{59}$$

$$N^{\text{idling},4}_{u,d}(k_d)=q_{u,d}(k_d) \tag{60}$$

$$N^{\text{dec}}_{u,d}(k_d)=(c_d-g^{\text{d}}_{u,d}(k_d))\alpha^{\text{arriv}}_{u,d}(k_d) \tag{61}$$

$$N^{\text{acc}}_{u,d}(k_d)=g^{\text{s}}_{u,d}(k_d)\mu_{u,d} \tag{62}$$

$$N^{\text{nonstop}}_{u,d}(k_d)=g^{\text{d}}_{u,d}(k_d)\alpha^{\text{arriv}}_{u,d}(k_d)\,, \tag{63}$$

and the time periods that the vehicles keep having this behavior in link (u,d) are given by

$$t^{\text{free}}_{u,d}(k_d)=c_d \tag{64}$$

$$t^{\text{idling},1}_{u,d}(k_d)=0 \tag{65}$$

$$t^{\text{idling},2}_{u,d}(k_d)=c_d-g^{\text{d}}_{u,d}(k_d)-(v_{\text{low}}-v_{\text{free}})/a_{\text{dec}} \tag{66}$$

$$-(v_{\text{free}}-v_{\text{low}})/a_{\text{acc}} \tag{67}$$

$$t^{\text{idling},3}_{u,d}(k_d)=0 \tag{68}$$

$$t^{\text{idling},4}_{u,d}(k_d)=c_d-g^{\text{d}}_{u,d}(k_d)-(v_{\text{free}}-v_{\text{low}})/a_{\text{acc}} \tag{69}$$

$$t^{\text{dec}}_{u,d}(k_d)=(v_{\text{low}}-v_{\text{free}})/a_{\text{dec}} \tag{70}$$

$$t^{\text{acc}}_{u,d}(k_d)=(v_{\text{free}}-v_{\text{low}})/a_{\text{acc}} \tag{71}$$

$$t^{\text{nonstop}}_{u,d}(k_d)=g^{\text{d}}_{u,d}(k_d)\,. \tag{72}$$

V. Objective function

Due to (7), for a given k_d (a counter for simulation time steps for node $d\in J$), the corresponding value of k_{c} is given by $k_{\text{c}}(k_d)=\lfloor k_d/N_d\rfloor$, where $\lfloor x\rfloor$ for x a real number denotes the largest integer less than or equal to x. On the other hand, a given value k_{c} of the control time step corresponds to the set $\{k_{\text{c}}N_d, k_{\text{c}}N_d+1,\cdots,(k_{\text{c}}+1)N_d-1\}$ of simulation time steps.

The objective function of the integrated urban control problem at control time step k_{c} is

$$J(k_{\text{c}})=\sum_{\theta\in\Theta}\frac{\lambda_\theta}{J_{\theta,\text{nominal}}}\sum_{(u,d)\in L}\sum_{k_d=N_dk_{\text{c}}+1}^{N_d(k_{\text{c}}+N_{\text{p}})}E_{\theta,u,d}(k_d)\,, \tag{73}$$

where $E_{\theta,u,d}(k_d)$ denotes the estimate partial criterion for θ in link (u,d) at simulation time step k_d, $\Theta=\{\text{TTS},\text{CO},\text{NO}_x,\text{HC},\text{CO}_2\}$ is the set of the control objectives, $J_{\theta,\text{nominal}}$ is the nominal performance for objective $\theta\in\Theta$ to normalize the partial objective of θ, and λ_θ is the weight parameter for objective θ. For the Total Time Spent (TTS), we have

$$E_{\text{TTS},u,d}(k_d)=T_{\text{s}}\cdot n_{u,d}(k_d)\,, \tag{74}$$

and (16) will be used for emissions (i.e. for $\theta\neq$ TTS). The goal of the control problem is to reduce the combined performance of the Total Time Spent and the variety of traffic emissions (i.e. CO, NO_x, HC, and CO_2) of the whole urban traffic network over the entire prediction horizon. Hence, it turns out to be a multiple objective control problem.

VI. MPC Controller For Urban Traffic Network

MPC [7] is a predictive control strategy that tries to find control inputs for the future. It has the ability to deal with the uncertainty of the process, which can be caused by the unpredictable disturbances, the (slow) variation over time of the parameters, or model mismatches in the prediction model. MPC can also easily deal with multi-input and multi-output problems with constraints. Another advantage of MPC is that one can easily select and replace the prediction model based on the control requirements. The MPC control process can be described by the following steps:

1) **Prediction model**. A model can be selected as prediction model for MPC controller, if it can predict the future traffic states. So the integrated VT-S model can be used as the prediction model of the MPC controller.
2) **Optimization problem**. Given the control interval T_{c} and the prediction horizon N_{p}, the optimization problem of MPC with a multi-objective function (as shown in (73)) can be expressed as

$$\begin{aligned} &\min_{\mathbf{g}(k_{\text{c}})} J=J(k_{\text{c}})\\ &s.t.\quad \text{Prediction model}\\ &\qquad \Phi(\mathbf{g}(k_{\text{c}}))=0\quad(\text{cycle time constraints})\\ &\qquad g_{\min}\le\mathbf{g}(k_{\text{c}})\le g_{\max} \end{aligned} \tag{75}$$

where $\mathbf{g}(k_{\text{c}})$ is the future control input at control step k_{c} (e.g. the green time), i.e. $\mathbf{g}(k_{\text{c}})=[g^{\text{T}}(k_{\text{c}}|k_{\text{c}})\ g^{\text{T}}(k_{\text{c}}+1|k_{\text{c}})\cdots\ g^{\text{T}}(k_{\text{c}}+N_{\text{p}}-1|k_{\text{c}})]^{\text{T}}$, and vector $g(k_{\text{c}}+j|k_{\text{c}})$ denotes the control input at the j th control step in the future from the current control time step k_{c}. To decrease the on-line computational complexity, a

control horizon N_c ($N_c < N_p$) can be defined, such that $g(k_c+i|k_c) = g(k_c+N_c-1|k_c)$ for $i = N_c, \cdots, N_p-1$. This nonlinear optimization problem can be solved by Sequential Quadratic Programming (SQP) algorithm.

3) **Rolling horizon**. The optimal control input $\mathbf{g}^*(k_c)$ is derived from the optimization, the first sample of the optimal results, $g^*(k_c \mid k_c)$, is implemented in the process. When arriving to the next control step, the prediction model is fed with real measured traffic states, the whole prediction horizon is shifted one step forward, and the optimization starts over again.

VII. Simulations

Now model predictive controllers for urban traffics are designed to reduce both TTS and TE (Total Emissions). To illustrate the effectiveness of the controllers, they are compared with a fixed-time controller. Given different weights to the partial objective functions, the MPC controller can emphasize on different traffic issues, and focus on improving different performance indications. Therefore, in the simulations, TTS and TE are respectively selected as the objective functions of the MPC controller. As for TE, the emissions for CO, CO_2, NO_x, HC are assigned equal weights. The performance of TTS and the emissions for CO, CO_2, NO_x, HC is listed in Table I for different controllers.

TABLE I
Performance for a Fixed-time Controller (FT) and for MPC Controllers Taking TTS and TE as Objective Function

Performances	FT	TTS-MPC	TE-MPC
TTS (veh·h)	1405	1244	1245
CO (kg)	35.80	22.91	22.84
CO_2 (kg)	11186.1	9283.2	9240.4
NO_x (kg)	4.32	3.45	3.40
HC (kg)	3.55	2.96	2.83

In Table I, the MPC controllers obtain better performance for both TTS and the emissions. For the MPC controllers, the TTS-MPC gets a lower TTS, but has higher emissions compared with TE-MPC; for TE-MPC, the reverse situation holds. However, the differences in performance are not big for TTS-MPC and TE-MPC. The reason for this phenomenon is that the curve of the vehicle emission model within the urban speed range [0,50] km/h is almost monotonously decreasing, except when $a = 1\,\mathrm{m/s^2}$. Therefore, the faster vehicles run, the less emissions will be released. But, in some circumstances, the environmental protection standard is stricter for some special regions, like resident area, school area, etc. Hence, more attention needs to be payed in these areas. To meet the high environmental standards for some local regions in urban areas, extra hard constraints or special high weights for the objective function can be defined in the MPC controllers to make sure the emissions are controlled below certain levels for these particular regions.

VIII. Conclusions

An integrated MPC controller for urban areas is established to reduce both travel delays and various types of traffic emissions based on a new proposed traffic model. The VT-micro emission model for individual vehicles is selected, and integrated with a macroscopic urban traffic flow model, the S-model, so as to form an integrated macroscopic urban traffic flow and emission model. The microscopic emission model guarantees that the emissions are correctly estimated for individual vehicles at different operational states. Moreover, after the emission model is integrated with a macroscopic model, the prediction model can still keep the computational efficiency of a macroscopic model for control purposes. Taking this model as the prediction model, MPC controller can address problems with multiple objectives with respect to both travel delays and emissions. The simulation results show that the MPC controller can reduce both total time spent and total emissions.

In the future, control problems aiming at keeping traffic emissions at certain regions under a predefined standard will be addressed. Fuel consumption will be also integrated into the controller. Further analysis will be performed for the urban traffic control problem through case studies using microscopic simulator and real traffic data.

IX. Acknowledgments

Research supported by a Chinese Scholarship Council (CSC) grant, the National Science Foundation of China (Grant No. 60674041, 60934007), the EU COST Action TU0702, the EU project "Hierarchical and distributed model predictive control (HD-MPC)", the Delft Research Center Next Generation Infrastructures, and the Transport Research Centre Delft.

References

[1] S. Zegeye, B. De Schutter, H. Hellendoorn, and E. Breunesse, "Reduction of travel times and traffic emissions using model predictive control," in *Proc. of the 2009 American Control Conference*, St. Louis, Missouri, June 2009, pp. 5392–5397.

[2] K. Ahn, A. A. Trani, H. Rakha, and M. Van Aerde, "Microscopic fuel consumption and emission models," in *Proc. of the 78th Annual Meeting of the Transportation Research Board*, Washington DC, USA, Jan. 1999, CD-ROM.

[3] M. C. Coelho, T. L. Farias, and N. M. Rouphail, "Impact of speed control traffic signals on pollutant emissions," *Transportation Research Part D*, vol. 10, no. 4, pp. 323–340, July 2005.

[4] ——, "Effect of roundabout operations on pollutant emissions," *Transportation Research Part D*, vol. 11, no. 5, pp. 333–343, Sept. 2006.

[5] S. Zegeye, B. De Schutter, J. Hellendoorn, and E. Breunesse, "Model-based traffic control for the reduction of fuel consumption, emissions, and travel time," in *Proc. of mobil.TUM 2009 — International Scientific Conference on Mobility and Transport*, Munich, Germany, May 2009.

[6] S. Zegeye, B. De Schutter, H. Hellendoorn, and E. Breunesse, "Model-based traffic control for balanced reduction of fuel consumption, emissions, and travel time," in *Proc. of the 12th IFAC Symposium on Transportation Systems*, Redondo Beach, California, Sept. 2009, pp. 149–154.

[7] J. Rawlings and D. Mayne, *Model Predictive Control: Theory and Design*. Madison, Wisconsin: Nob Hill Publishing, 2009.

[8] S. Lin, B. De Schutter, Y. Xi, and J. Hellendoorn, "A simplified macroscopic urban traffic network model for model-based predictive control," in *Proc. of 12th IFAC Symposium on Control Transportation Systems*, Redondo Beach (CA), USA, 2009, pp. 286–291.

[9] ——, "Study on fast model predictive controllers for large urban traffic networks," in *Proc. of 12th International IEEE Conference on Intelligent Transportation Systems*, St. Louis (MO), USA, 2009, pp. 691–696.